Applied and Environmental Microbiology, Sept. 2011, p. 6419–6425 Vol. 77, No. 18
0099-2240/11/$12.00 doi:10.1128/AEM.05219-11

Self-Inducible *Bacillus subtilis* Expression System for Reliable and Inexpensive Protein Production by High-Cell-Density Fermentation▽†

Marian Wenzel,[1] Alexander Müller,[2] Martin Siemann-Herzberg,[2] and Josef Altenbuchner[1]*

Institut für Industrielle Genetik, Universität Stuttgart, Allmandring 31, 70569 Stuttgart, Germany,[1] and Institut für Bioverfahrenstechnik, Universität Stuttgart, Allmandring 31, 70569 Stuttgart, Germany[2]

Received 20 April 2011/Accepted 20 July 2011

A novel technically compliant expression system was developed for heterologous protein production in *Bacillus subtilis* with the aim of increasing product yields at the same time as decreasing production costs. Standard systems involve the positively regulated *manP* promoter of the mannose operon, which led to relatively high product yields of 5.3% (5.3 g enhanced green fluorescent protein [eGFP] per 100 g cell dry weight [CDW]) but required large quantities of mannose to induce the reactions, thus rendering the system's technical application rather expensive. To improve this situation, mutant *B. subtilis* strains were used: the Δ*manA* (mannose metabolism) strain TQ281 and the Δ*manP* (mannose uptake) strain TQ356. The total amount of inducer could be reduced with TQ281, which, however, displayed sensitivity to mannose. An inducer-independent self-induction system was developed with TQ356 to further improve the cost efficiency and product yield of the system, in which glucose prevents induction by carbon catabolite repression. To create optimal self-induction conditions, a glucose-limited process strategy, namely, a fed-batch process, was utilized as follows. The initiation of self-induction at the beginning of the glucose-restricted transition phase between the batch and fed-batch phase of fermentation and its maintenance throughout the glucose-limiting fed-batch phase led to a nearly 3-fold increase of product yield, to 14.6%. The novel *B. subtilis* self-induction system thus makes a considerable contribution to improving product yield and reducing the costs associated with its technical application.

The Gram-positive soil bacterium *Bacillus subtilis* is an attractive host for the production of various industrial proteins, such as amylases, proteases, and lipases. It is classified as a generally recognized as safe (GRAS) organism due to its lack of pathogenicity and absence of endotoxins. Further advantages of *B. subtilis* are its direct secretion of proteins into the medium via the Sec and Tat protein secretion machineries (40), capacity for genetic manipulation, easy handling, short processing times, and application in large-scale industrial production of proteins, for example, laundry enzymes and riboflavin (34). Homologous proteins can be produced in the order of several grams per liter, but only a few milligrams per liter of proteins can be produced from heterologous sources (34, 35). When it comes to the biotechnological production of heterologous proteins, care must be taken to enable the reliable and inexpensive production of high yields of desired proteins. Priority was given to the development of a novel, technically compliant bacterial gene expression system that would be both cheap and highly reliable. Regulated promoters used in expression vectors can be induced by sugars, isopropyl-β-D-thiogalactopyranoside (IPTG), temperature shifts, acid shock, or ethanol (27, 28, 29, 35). If such systems are to be technically exploited, ways need to be found to circumvent the high price of inducers required. Autoinducible systems stand to improve this situation. However, until now, only a few natural autoinducible *B. subtilis* systems have been known, e.g., the *pst* operon, the *gsiB* promoter, and the lysine riboswitch (35). Artificial autoinduction can also be achieved by using growth phase- or stress-specific promoters that depend on the activity of alternative sigma factors (23, 35). To our knowledge, none of these have yet been tested and approved for high-cell-density fermentations with *B. subtilis*.

The *B. subtilis* mannose operon consists of three genes, *manP*, *manA*, and *yjdF* (20) (Fig. 1). *manP* encodes the phosphotransferase system (PTS) mannose-specific enzyme IIBCA which belongs to the Fru-permease family (32), and *manA* encodes a mannose 6-phosphate isomerase which converts the incoming mannose 6-phosphate to fructose 6-phosphate that subsequently enters glycolysis. The function and affiliation of *yjdF* are not yet known. The *manR* gene, which is located upstream and in the same orientation as the mannose operon, encodes the transcriptional activator of the mannose operon (31, 38). Similar to the *Geobacillus stearothermophilus* MtlR, ManR harbors a DNA binding motif at the N-terminal end, two PRDs (PTS regulation domain), PRD1 and PRD2, and an EIIB- and EIIA-like domain (9).

The mannose operon possesses a relatively strong and tightly regulated promoter (38). *B. subtilis* takes up mannose via the phosphoenolpyruvate:carbohydrate PTS and phosphorylates the substrate as it is translocated. The PTS consists of the general cytoplasmic protein enzyme I (EI), the histidine protein (HPr), and the substrate-specific membrane protein enzyme II (EII). The latter represents a sugar-specific permease consisting of three (EIIABC) or four (EIIABCD) subunits which are either multidomain proteins or separate individual polypeptides (4, 5, 30).

* Corresponding author. Mailing address: Institut für Industrielle Genetik, Universität Stuttgart, Allmandring 31, 70569 Stuttgart, Germany. Phone: 49 711 685 67591. Fax: 49 711 685 66973. E-mail: josef.altenbuchner@iig.uni-stuttgart.de.

† Supplemental material for this article may be found at http://aem.asm.org/.

▽ Published ahead of print on 29 July 2011.

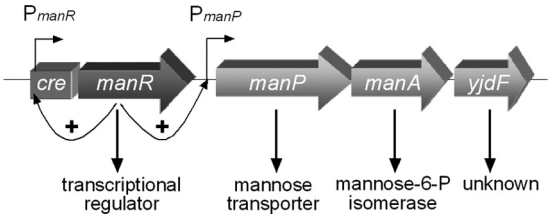

FIG. 1. Schematic representation of the *B. subtilis* mannose operon. The genes are shown as thick arrows, the two promoters as thin arrows above the genes, and the *cre* site near the P_{manR} as a box. The positive regulatory effect (plus sign) of ManR on the two promoters is indicated.

To adapt quickly to available carbon and energy sources, the bacterial mannose operon is upregulated in the presence of mannose and repressed by glucose, called carbon catabolite repression (CCR). In analogy to the *B. subtilis* MtlR and other PRD-containing activators (13, 14, 15), we can assume at present that the EIIA and EIIB domains of ManR are phosphorylated by the ManP transporter in the absence of mannose and dephosphorylated in its presence. The PRD2 domain of ManR is phosphorylated in the presence of glucose and dephosphorylated in its absence. ManR is only active when the EIIAB domains are dephosphorylated and PRD2 is phosphorylated, which explains the induction by mannose and catabolite repression by glucose (Fig. 2). In addition, a second CCR mechanism exists, which is exerted by HPr on the expression of *manR*. The presence of glycolytic intermediates, such as glucose 6-phosphate or fructose 1,6-bisphosphate, induces HPr kinase to phosphorylate HPr at Ser46, whereupon P-Ser46-HPr binds to CcpA (catabolite control protein) (5, 6, 8, 10, 12, 25, 41, 42). The resulting complex can bind to the operator sequence *cre* (catabolite responsive element) located in front of catabolic genes to prevent the transcription of the target operons (7, 44). Such a *cre* site is located in front of the *manR* gene (38). Deletion of the *manP* gene leads to the constitutive expression of the mannose operon even in the absence of mannose. Nevertheless, the *manP* promoter can still be regulated by glucose and lead to CCR (38).

High-cell-density culture conditions were adapted for stringent, CCR-controlled heterologous gene expression. The initial batch phase in a fed-batch fermentation is characterized by

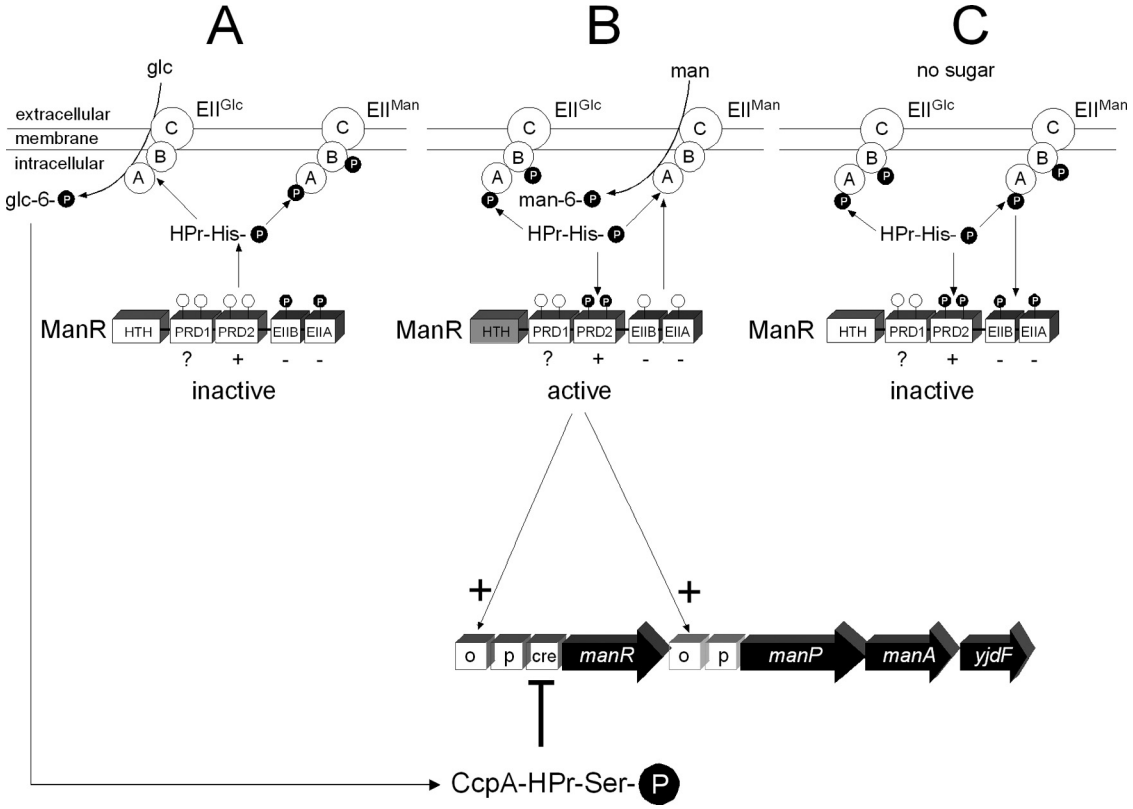

FIG. 2. Model of PTS-mediated control of ManR. The domain structure of ManR is shown along with its putative phosphorylation sites (open circles) and the functions of these domains (?, unknown; +, activating; −, deactivating). Phosphoryl groups are indicated as black circles with a white "P." The mannose operon, including the binding sites for ManR (o, operator), CcpA-HPr-His-P (*cre*), and the promoters (p), is shown. (A) Glucose (glc) is taken up and phosphorylated by EII^{Glc}. The PRD2 of ManR becomes dephosphorylated by HPr, while the EII domains remain phosphorylated. ManR is inactive and cannot bind to its operator sequences. Rising intracellular levels of glucose 6-phosphate (glc-6-P) and other metabolites lead to the formation of CcpA-HPr-His-P, a complex that acts as a repressor by binding to the *cre* site. No expression from the mannose operon promoters takes place. (B) When the inducer mannose is available, it is taken up and phosphorylated by its cognate EII^{Man}. HPr phosphorylates the PRD2, and the EII domains transfer their phosphoryl groups to EII^{Man}. ManR is active, and expression from the mannose promoters takes place. (C) When no sugar is available, all PTS components, as well as the PRD2 and EIIB- and EIIA-like domains of ManR, are present in a phosphorylated state. ManR is not active, and no expression from the mannose operon promoters takes place.

TABLE 1. List of oligonucleotides

Oligonucleotide	Sequence (5′ → 3′)
P1	AAAAAATGATCAACCGGTCGATTGCCACATTA
P2	CATATGTATATCTCCTTCTTAAGAAAATTATTTCTAGAAAGT
P3	ACTTTCTAGAAATAATTTTCTTAAGAAGGAGATATACATATG
P4	AAAAAATGATCATTACTTGTACAGCTCGTCCAT
P5	AAAAAAGAATTCGAGATCAGGGAATGAGTTTATA
P6	AAAAAACCGCTCGTCTTCCTAAGCATCCTTCAA
P7	TTAAGAATTAAAGGAGGAATTCAAAATGGCAGACAATAACAAAG
P8	GATCCTTTGTTATTGTCTGCCATTTTGAATTCCTCCTTTAATTC

an excess of nutrients, namely, glucose. This specifically enables strong catabolite repression of CCR-responsive promoters. The subsequent fed-batch phase is then achieved based on controlled substrate limitation with glucose as the sole carbon source. This feeding strategy is a prerequisite for obtaining high cell densities (24), since it leads to reduced specific growth rates and (consequently) to diminished oxygen consumption rates. The excess glucose during the initial batch phase and (caused by the applied feed rate) "forced" carbon limitation during the fed-batch phase are aligned to an inducible catabolite repression-dependent expression system. These systems are known to be tightly regulated with respect to their inducibility and low background titers (45). The novel *B. subtilis* expression system based on the mannose operon proves to be suitable for application in high-cell-density fermentations. The technically compliant system was approved and further optimized to the point of a highly efficient self-induction system in order to reduce operational expenses.

MATERIALS AND METHODS

Bacterial strains and growth conditions. *E. coli* JM109 (46) was used as a host for cloning experiments. *B. subtilis* strains 3NA (*spo0A*) (26), TQ281 (*spo0A* Δ*manA::ermC*), and TQ356 (*spo0A* Δ*manP::ermC*) (38) were used for fermentation experiments.

Strains were grown at 37°C in LB medium (1). The selection conditions were as follows: ampicillin, 100 μg ml^{-1}; spectinomycin, 100 μg ml^{-1}; and erythromycin, 5 μg ml^{-1}. *E. coli* JM109 was transformed with plasmid DNA using the TSS (transformation and storage solution) method (3). *B. subtilis* strains were transformed with plasmid DNA according to the modified "Paris method" (11).

Materials. All chemicals (analytical grade) were purchased from Sigma-Aldrich Corporation (Taufkrichen, Germany) and Merck KGaA (Darmstadt, Germany). Synthetic DNA oligonucleotides (Table 1) were purchased from Eurofins MWG Operon GmbH (Ebersberg, Germany). Restriction enzymes and DNA-modifying enzymes were purchased from Roche Diagnostics Deutschland GmbH (Mannheim, Germany) or New England BioLabs GmbH (Frankfurt am Main, Germany). PCRs were run with Phusion high-fidelity DNA polymerase from Fermentas GmbH (St. Leon-Rot, Germany) on a MiniCycler from MJ Research, Inc. (Waltham, MA).

Construction of expression vector pMW168.1. The central expression vector pMW168.1 (Fig. 3) used in this study comprised the replication regions for *Escherichia coli* and *B. subtilis*, one common resistance marker, and the expression cassette consisting of an enhanced green fluorescent protein (eGFP) gene under the control of the strong *manP* promoter flanked by transcriptional terminators. Standard recombinant DNA techniques were used for cloning experiments (33). Originating from the *E. coli lacZ* expression vector pSUN252.1 (38), the *lacZ* gene was excised with BamHI, resulting in pSUN266.1. The spectinomycin resistance gene *aad9* (22), as well as the two cloning sites BamHI and SmaI which are flanked by two *B. subtilis tufA* transcription terminators (18), were inserted into EcoRI/HindIII-cut pUC18 (46) by cutting pSUN266.1 with MunI/HindIII, resulting in pMW93.1. Plasmid pMW104.2 was created by removing the ampicillin resistance gene (*bla*) by deleting a BspHI/SfoI fragment from pMW93.1. The expression cassette with eGFP was put under the control of the promoter of the *manPA* operon (P_{manP}) (38) by inserting it into the BamHI restriction site, resulting in pMW115.1. This expression cassette was constructed by fusing the P_{manP} promoter region of plasmid pSUN284.1 (38) to the eGFP gene of plasmid pWA21 (43) at the AflII site. The fusion was conducted via PCR amplification of the two fragments using oligonucleotide primers P1/P2 and P3/P4, respectively. The cassette was cut with BclI before ligation with pMW104.2. To generate a shuttle vector capable of replicating in both *E. coli* and *B. subtilis*, the pUB110 (17) replicon comprising the *rep* gene and *ori*$^+$ were PCR amplified using primers P5/P6 and inserted in EcoRI/BsrBI-digested pMW115.1. The translational initiation region was replaced with that of *gsiB* (16), including the ribosomal binding site, the start codon, and the following six codons of *gsiB*. Thereafter, the complementary oligonucleotides P7/P8 were used to replace the region between the restriction sites AflII/BamHI to give pMW168.1.

Composition of media used for fermentation. Overnight culture and preculture number 1 were carried out in Spizizen's minimal salts medium (SMM) (36) supplemented with 0.02% (wt/vol) Casamino acids (BD Difco, Sparks, MD) and 100 μg ml^{-1} spectinomycin for plasmid selection and 5 μg ml^{-1} erythromycin for strain selection (for TQ281 and TQ356). Preculture number 2 and the fermentation culture (batch) were carried out using a mineral salt medium modified from that of Wilms et al. (45), consisting of 1.0 g liter^{-1} $(NH_4)_2$-H-citrate, 2.0 g liter^{-1} Na_2SO_4, 2.68 g liter^{-1} $(NH_4)_2SO_4$, 0.5 g liter^{-1} NH_4Cl, 14.6 g liter^{-1} K_2HPO_4, 4.0 g liter^{-1} $NaH_2PO_4 \times H_2O$, 1.0 g liter^{-1} $MgSO_4 \times 7\ H_2O$, 3 ml liter^{-1} trace element solution (TES) with 5 g liter^{-1} glucose for preculture number 2 and 25 g liter^{-1} glucose for the batch medium. TES contains 0.5 g liter^{-1} $CaCl_2$, 0.18 g liter^{-1} $ZnSO_4 \times 7\ H_2O$, 0.1 g liter^{-1} $MnSO_4 \times H_2O$, 10.05 g liter^{-1} Na_2-EDTA, 8.35 g liter^{-1} $FeCl_3$, 0.16 g liter^{-1} $CuSO_4 \times 5\ H_2O$, and 0.18 g liter^{-1} $CoCl_2 \times 6\ H_2O$. The feed medium for high-cell-density fermentations contained 200 g liter^{-1} glucose, 7.89 g liter^{-1} $MgSO_4 \times 7\ H_2O$, 40 ml liter^{-1} of TES, and 63.36 g liter^{-1} $(NH_4)_2HPO_4$ when a KLF reactor was used. The pH was adjusted to 3.3 to ensure the solubility of all components. Two separate feed media were used when a 30-liter reactor was used. The first medium contained 654.76 g liter^{-1} glucose $\times H_2O$, 23.5 g liter^{-1} $MgSO_4 \times 7\ H_2O$, 120 ml liter^{-1} TES, and the second 396 g liter^{-1} $(NH_4)_2HPO_4$. For induction of the *manP* promoter, either 20% (wt/vol) D-mannose solution or a separate feeding solution containing 200 g liter^{-1} mannose, 7.89 g liter^{-1} $MgSO_4 \times 7\ H_2O$, 40 ml liter^{-1} TES, and 63.36 g liter^{-1} $(NH_4)_2HPO_4$ was used.

Preculture and fed-batch cultivation conditions. Single colonies from LB agar plates were inoculated in 5 ml of SMM and incubated overnight for at least 14 h at 37°C. Amounts of 25 ml of SMM were transferred to 250-ml shaking flasks and

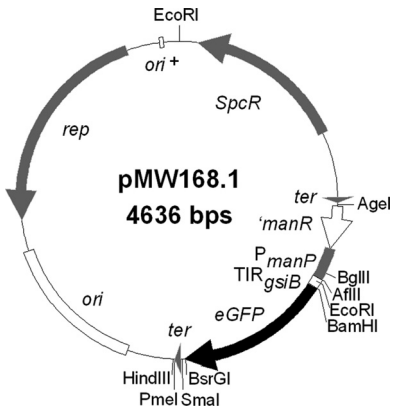

FIG. 3. Physical map of the expression vector pMW168.1. The following genes (arrows) and regions (boxes) are shown: SpcR (*aad9*), spectinomycin resistance gene; *ter*, transcriptional terminator from *tufA*; '*manR*, 5′-truncated form of *manR*; P_{manP}, promoter region from *manPA* operon; TIR_{gsiB}, translational initiation region from gene *gsiB*; *eGFP*, enhanced green fluorescent protein gene; *ori*, origin of replication from pUC18; *rep* and *ori*$^+$, *rep* gene (initiator protein) and *ori*$^+$ from pUB110.

inoculated with the overnight culture to achieve an optical density at 600 nm (OD_{600}) of 0.05 (preculture number 1). After 5 h of incubation at 37°C, 20-ml amounts of preculture number 1 were used to inoculate 200 ml of preculture number 2 medium in 1,000-ml shaking flasks (preculture number 2). After another 7 h of incubation at 37°C, the batch culture medium was inoculated with preculture number 2.

A fed-batch fermentation setup previously developed and optimized for *E. coli* with glucose as the main carbon source was used (19, 45). The batch volume was 1.5 liters and the feeding volume 1.0 liter when a 3.7-liter KLF small laboratory fermenter (Bioengineering AG, Wald, Switzerland) was used. In the case of a 30-liter D598 laboratory fermenter (LF; Bioengineering AG, Wald, Switzerland), the batch volume was 8.0 liters, the glucose feed medium 4.2 liters, and the ammonia feed medium 1.0 liter. Glucose and ammonia media were fed into the reactor in an 81%:19% ratio. The feed media were fed into the bioreactor according to the equation $F(t) = [(\mu_{set}/Y_{X/S}) + m] \times [(c_{x0} \times V_0)/c_{s0}] \times \exp(\mu_{set} \times t)$, where F (liter h^{-1}) is the feeding rate, μ_{set} (h^{-1}) is the desired specific growth rate, m (g g^{-1} h^{-1}) is the specific maintenance coefficient (0.04 g g^{-1} h^{-1}), $Y_{x/s}$ is the specific biomass/substrate yield coefficient (approximately 0.5 for glucose), c_{x0} (g $liter^{-1}$) is the biomass concentration at start of feeding, V_0 (liter) is the reactor volume at start of feeding, c_{s0} (g $liter^{-1}$) is the glucose concentration in the feeding solution, and t (h) is the time after start of feeding. A specific growth rate μ of 0.1 h^{-1} was chosen to avoid the production of nonspecific and unwanted by-products and to avoid oxygen limitation.

The batch cultivation was carried out at 37°C until the temperature was shifted to 30°C at the beginning of the fed-batch phase to avoid unwanted inclusion body formation of the expressed heterologous protein. The pH was adjusted to 7.0 with 24% (vol/vol) NH_4OH and 20% (vol/vol) H_3PO_4. The partial oxygen pressure (pO_2) value was maintained at over 50% saturation by an automatically adjusting stirrer speed. The aeration rate was kept constant at 2 liters min^{-1} when using the KLF and between 15 and 25 liters min^{-1} when using the LF. The overpressure was kept at 0.5 bar. The cell density was determined by measuring the OD_{600} periodically with an Ultrospec 1100 *pro* UV/visible light spectrophotometer (GE Healthcare, formerly Amersham Biosciences, United Kingdom). The cell dry weight (CDW) was calculated by multiplying the OD_{600} value by a factor of 0.322 g CDW $liter^{-1}$, which was obtained as an average value after several moisture determinations with an MB 835 halogen (Ohaus Corporation, Pine Brook, NJ) during the fermentations. The Biolog 1.7 software package (Institute of Biochemical Engineering, University of Stuttgart, Germany [http://www.ibvt.uni-stuttgart.de]) was used for controlling the fermentation parameters. The fed-batch fermentations were terminated after approximately 40 h of process time.

Online and offline fluorescence measurements. To track the expression rate of the recombinant eGFP in real time, a fluorescence probe (Mikropack HPX-2000 high-power xenon light source and S2000 fiber optic spectrometer; Ocean Optics, Inc., Dunedin, FL) was used inside the bioreactor. The excitation wavelength was 485 nm, while the emission was detected at 535 nm and recorded online using the Spectra Suite software package (Ocean Optics, Dunedin, FL). The fluorescence light was channeled through an optic filter with a strength of 0.6. The integration time of the probe was 50 ms. Because of the fact that the software was only able to count values up to 4,000 counts, the integration time was reduced stepwise just before reaching higher levels. Hence, the fluorescence counts were multiplied afterwards by the corresponding reduction factor to get the values which correspond to 50 ms. The measured values were specific for a certain reactor volume.

Additionally, offline measurements of fluorescent activity were conducted by using a SpectraFluor microplate reader (Tecan Group Ltd., Männedorf, Switzerland). Therefore, 3 250-μl amounts of undiluted cell culture were measured in 96-well microplates (Greiner-Bio One GmbH, Frickenhausen, Germany) using 3 250-μl amounts of batch medium as the blank value (excitation filter, 485 nm; emission filter, 535 nm; gain [manual], 60; integration time, 20 μs; number of flashes, 3; read mode, top). The average of the blank values was subtracted from the average of the samples to get the final value. The cell culture was diluted in batch medium as soon as 20,000 counts were reached.

From a calibration against an internal purified eGFP standard (approximately 95% purity, 1.3 g $liter^{-1}$), it could be conveyed that about 120,000 offline measured counts correspond to 1 g eGFP $liter^{-1}$. It could be shown that a linear coherence exists between the offline and online measured values which gave a correlation of 1.5 g eGFP $liter^{-1}$ per 7,470 online measured counts.

Protein analysis by SDS-PAGE. Crude cell extracts were obtained as follows. The OD_{600} was measured, and a certain volume corresponding to approximately 10^{10} cells was harvested and centrifuged. The pelleted cells were resuspended with 1 ml 50 mM sodium phosphate buffer (pH 7.5), and crude cell extract prepared using ultrasonic sound (3 times for 30 s, 50% duty cycle using a model W-385 sonicator; Heat Systems-Ultrasonics, Inc., Farmingdale, NY). The crude cell extract was separated into a soluble (supernatant) and insoluble protein fraction (pellet) by centrifugation. The material of the insoluble fraction was obtained by resuspending the pellet with 1 ml 50 mM sodium phosphate buffer (pH 7.5). The protein fractions were analyzed by SDS-PAGE (21, 33).

RESULTS

Setup of the mannose expression system in *B. subtilis*. Previous experiments have shown that the *manPA-yjdF* operon possesses a strong promoter, P_{manP}, that can be used for expression purposes (38). An expression vector, pMW168.1, with an eGFP gene under the control of P_{manP} was constructed (Fig. 3). This shuttle vector carries the pUC18 origin of replication for *E. coli* and the pUB110 *rep* gene and *ori*$^+$ for replication in *B. subtilis*. A spectinomycin resistance gene, *aad9*, from *Enterococcus faecalis* was used as a common selection marker to minimize the size of the vector. Further improvement of the expression level could be achieved by replacing the original translational initiation region (TIR) with that of *gsiB* (16).

The nonsporulating *B. subtilis* strain 3NA, with a mutation in the *spo0A* gene, was chosen for fermentation purposes to avoid sporulation during fermentation and the risk of spores persisting in the bioreactor. After transformation with pMW168.1, the strain showed high fluorescence activity after induction with mannose.

High-cell-density fermentations using *B. subtilis* 3NA/pMW168.1. The mannose expression system with *B. subtilis* 3NA/pMW168.1 was tested in fed-batch fermentations under conditions described previously (19, 45), with some modifications.

In the first fermentation, carried out in an LF stirring reactor, an amount of 0.2% (wt/vol) mannose was added to the culture broth immediately at the beginning of the fed-batch phase. The fluorescence signal of the probe, showing no significant fluorescence so far, increased very quickly right after induction. After reaching a peak value at about 2,200 counts after 4 h in the fed-batch phase, the signal began to decrease again steadily. This decrease was accompanied by the consumption of inducer (measured by high-performance liquid chromatography [HPLC], data not shown). At the end of the process, 0.2 g eGFP $liter^{-1}$ was produced, which corresponds to a product yield of 0.3% (0.3 g eGFP per 100 g CDW).

In a second fermentation, an additional exponential mannose feed was used. That was started simultaneously with the glucose feed, keeping the overall sugar concentration of both feeds as high as in the first fermentation. The fluorescence signal started right after the addition of inducer and was extended until the end of the process. An overall amount of 50 g mannose was added to the reactor broth to sustain this increase. With this induction regime, 2.1 g eGFP $liter^{-1}$ was produced, which corresponds to a product yield of 5.3% (5.3 g eGFP per 100 g CDW). Table 2 shows the detailed results of the two fermentations conducted with *B. subtilis* 3NA/pMW168.1.

The eGFP production increased throughout the whole fed-batch-phase but more slowly than the biomass production.

High-cell-density fermentation using the Δ*manA* strain TQ281. The *manA* deletion strain TQ281, which is incapable of growing on mannose as the sole carbon source (38), was cho-

TABLE 2. Comparison of fermentations (single performances) with regard to the different induction regimes and *B. subtilis* strains with expression vector pMW168.1[a]

B. subtilis strain with pMW168.1	Induction regime	Stirring reactor	Δt_{fb} (h)	μ_{fb} (h^{-1})	$c_{x,\ final}$ (g CDW $liter^{-1}$)	X_{final} (g CDW)	$c_{P,\ final}$ (g eGFP $liter^{-1}$)	$P_{eGFP,\ final}$ (g)	$Y_{P/X}$ (%)	r_P (g eGFP g CDW^{-1} h^{-1})	q_P (g eGFP $liter^{-1}$ h^{-1})
3NA (*man*$^+$)	SA	LF	22.5	0.09	73	897	0.2	2.8	0.3	0.14×10^{-3}	0.01
3NA (*man*$^+$)	EF	KLF	23.8	0.09	39	103	2.1	5.5	5.3	2.32×10^{-3}	0.09
TQ281 (Δ*manA*)	SA	KLF	11.8	0.09	20	39	0.7	1.4	3.6	2.98×10^{-3}	0.06
TQ281 (Δ*manA*)	EF	LF	25.5	0.08	59	782	1.9	25	3.2	1.37×10^{-3}	0.08
TQ356 (Δ*manP*)	SI	LF	23.5	0.1	67	758	9.8	111	14.6	6.23×10^{-3}	0.40

[a] Abbreviations and parameter descriptions: SA, single addition of inducer (mannose); EF, exponential feeding of inducer (mannose); SI, self-induction; final, at the end of the fermentation process; LF, 30-liter laboratory fermenter; KLF, 3.7-liter small laboratory fermenter; Δt_{fb}, fed-batch time/duration; μ_{fb}, average specific growth rate in the fed-batch phase; $c_{x,\ final}$, cell dry weight concentration; X_{final}, absolute cell dry weight; $c_{P,\ final}$, product concentration; $P_{eGFP,\ final}$, absolute product (eGFP); $Y_{P/X}$, product yield in g eGFP per 100 g CDW; r_P, specific productivity; q_P, volumetric productivity.

sen for further fermentation experiments. *B. subtilis* TQ281 transformed with pMW168.1 showed a growth defect in shaking flask experiments when mannose was present. The addition of the sugar led to growth inhibition and morphological changes.

Two fed-batch fermentations were set up with TQ281/pMW168.1. In the first one, induction took place by a single addition of mannose at the beginning of the fed-batch phase. In the second one, an additional exponential mannose feed was started at the same time. Induction with mannose showed no significant impact on the specific growth rate in the fed-batch phase (see Table 2). With the single-addition strategy, 0.71 g eGFP $liter^{-1}$ could be achieved, corresponding to a product yield of 3.6% (3.6 g eGFP per 100 g CDW), and with the exponential feeding strategy, 1.9 g eGFP $liter^{-1}$, corresponding to a product yield of 3.2% (3.2 g eGFP per 100 g CDW). The detailed results of the two fermentations are listed in Table 2.

Development and application of a self-inducible expression system in high-cell-density fermentation using the Δ*manP* strain TQ356. The *B. subtilis* Δ*manP* strain TQ356 showed constitutive expression from P_{manP} under noninductive conditions, as well as a CCR effect when glucose was present (38). That strain was transformed with pMW168.1, which led to rather small fluorescing colonies. After the addition of 0.5% (wt/vol) glucose to the selection media, colony growth was normalized. In shaking flask experiments, high expression levels were achieved, during which glucose was exhausted (data not shown).

B. subtilis TQ356 harboring pMW168.1 was then used for a fed-batch fermentation (Fig. 4). In the batch phase, no significant fluorescence could be detected, similar to the batch fermentation of *B. subtilis* strains 3NA/pMW186 and TQ281/pMW168. With the beginning of the fed-batch phase, the fluorescence signal of the reactor probe began to increase continuously. After 36 h overall fermentation time, the expression level in the cells reached a maximum, as can be seen by a constant $Y_{P/X}$ value of 14.6% until the end of the fermentation process, which corresponds to a constant specific productivity. Nearly 10 g eGFP $liter^{-1}$ were produced, corresponding to a product yield of 14.6% (14.6 g eGFP per 100 g CDW), without any addition of inducer. In Table 2, the fermentation results are summarized and compared to the other fermentations conducted in this study. SDS-PAGE was conducted to get an impression of the percentage of eGFP expressed in comparison to total protein (Fig. 5). As can be seen, at least 20% of total protein is eGFP molecules. Only a small fraction is insoluble and present in the form of inclusion bodies (Fig. 5, lane 7). Undiluted culture broth supernatant was also analyzed by SDS-PAGE (Fig. 5, lane 8) and measured spectrophotometri-

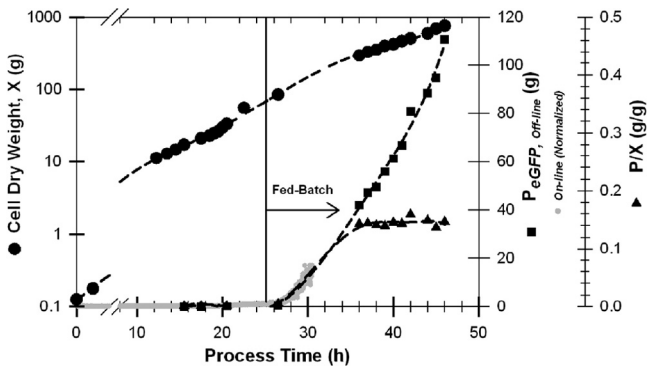

FIG. 4. Fed-batch fermentation of *B. subtilis* TQ356/pMW168.1. Cell dry weight (X, black circles), total amount of eGFP produced (P_{eGFP}, black squares), and product yield (P/X, black triangles) are plotted over the fermentation time. The beginning of the fed-batch phase is indicated by a vertical line.

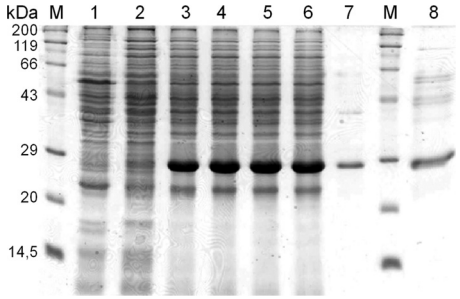

FIG. 5. SDS-PAGE of cell samples taken from the fermentation with *B. subtilis* TQ356/pMW168.1. Lanes: M, Roti-Mark Standard protein molecular mass marker; 1, soluble fraction after 12.5 h (batch); 2, soluble fraction after 20.5 h (batch); 3, soluble fraction after 36 h (13.5 h fed-batch); 4, soluble fraction after 41 h (18.5 h fed-batch); 5, soluble fraction after 44 h (21.5 h fed-batch); 6, soluble fraction after 46 h (23.5 h fed-batch, end of process); 7, insoluble fraction after 46 h; 8, culture supernatant after 46 h.

cally. Circa 1% of the total measured eGFP could be found in the supernatant.

DISCUSSION

A novel inducible *B. subtilis* expression system involving the mannose operon was developed and optimized for application in high-cell-density fermentations. The strong mannose promoter P_{manP} is activated upon the addition of mannose (38). That promoter was used in the vector pMW168.1 to promote the expression of eGFP. The *B. subtilis* sporulation-deficient strain 3NA, which was transformed with this vector, led to high product levels, i.e., 2.1 g eGFP liter^{-1}. Compared to a recently described system with *Bacillus megaterium* (37), a promising host system for recombinant protein production, the novel *B. subtilis* system leads to superior results. The intracellular *B. megaterium* protein production system, which is inducible by xylose, gave 1.25 g eGFP liter^{-1}, corresponding to a product yield of 3.7% (3.68 g eGFP per 100 g CDW) in fed-batch fermentations. In addition, Stammen et al. (37) used antibiotics until the end of the fermentation process, with the result that no plasmids were lost during the fermentation process.

Although the mannose system is rather efficient concerning productivity, a one-time addition of the inducer does not lead to permanent high expression rates. This is due to the rapid consumption of the inducer mannose, as it is one of the favorite carbon sources of *B. subtilis*. Additionally, mannose is a rather expensive sugar, making the expression system economically unfeasible for large-scale industrial applications.

In order to optimize the system for industrial applications, mannose catabolism must be avoided. This was achieved by disrupting the mannose 6-phosphate isomerase gene *manA*. That should lead to a minimum need of inducer molecules to gain high expression rates. Indeed, less inducer was needed, as could be observed in the shaking flask experiments. That system was accompanied by a self-toxification of the cells, since growth was inhibited when using amounts of over 0.5% (wt/vol) mannose. The cells showed severe morphological changes. That effect may be due to the intracellular accumulation of mannose 6-phosphate, which itself may lead to a high osmotic pressure, leading to the bubble-like cells which could be seen under the microscope. Another possible reason for the sensitivity of the Δ*manA* strain TQ281 to mannose may be the strong reduction of available phosphate groups, since phosphate is irreversibly bound to mannose when entering the cells via the PTS. However, TQ281/pMW168.1 used in fed-batch fermentations still required a considerable amount of the inducer mannose for optimal protein production.

That led us to the idea of generating an induction regime which no longer needs any inducer. That self-inducible system was put into effect with the Δ*manP* strain TQ356 and expression vector pMW168.1. Prior experiments have shown constitutive expression from the *manP* promoter (38). That observation was in concordance with the results published by Joyet et al. (15). The obvious role of the EII-like domains of the regulator led us to the following putative regulation mechanism (Fig. 2): ManP phosphorylates the EIIB- and EIIA-like domain of ManR when mannose is not available so that the regulator becomes inactive. In a transporter-negative strain like TQ356, the mannose promoter is only under regulatory control by the CCR that was dependent on glucose, which was the case for the batch phase of a fermentation process. The negative regulatory effect by the cognate transporter ManP is abolished. Nevertheless, the regulator stays in an inactive state as long as HPr transfers no phosphate to the PRD2 domain of ManR, which is the case in the presence of glucose. In addition, there are not sufficient amounts of ManR as long as CcpA-HPr-Ser46-P is blocking the *manR* operator site and ManR is inactive due to the dephosphorylated PRD2. Not until glucose becomes limiting ManR can bind to its operator sequence and start the expression. That self-induction system rendered the need for the rather expensive inducer mannose unnecessary. This induction strategy seems to be very promising for industrial applications, since no significant unwanted basal expression takes place in the batch phase and no addition of any inducer is necessary to obtain high levels of expression throughout the fed-batch phase. Nearly 10 g liter^{-1} of recombinant protein (eGFP), corresponding to a product yield of 14.6%, could be achieved. The product was homogeneously distributed in the cells due to its solubility, as could be observed by fluorescence microscopy and SDS-PAGE analysis.

Plasmids replicating by a rolling-circle replication mechanism, like pUB110 used in this study for vector construction, are known to be structurally and segregationally unstable (2). No structural instability has been seen with pMW168.1 so far. The plasmid stability of 3NA/pMW168.1 was tested in shaking flask cultures in LB liquid medium without antibiotic selection. Within 65 generations, about 90% of the cells had lost the plasmid. However, about 5% of cells had lost the plasmid within the first 20 generations, which is the relevant number for fed-batch fermentations (see Fig. S2 in the supplemental material), and the productivity could be maintained at a high, constant level until the end of the fermentation process (Fig. 4). In addition, no antibiotic selection pressure was necessary to obtain high expression rates and productivities in any of the fermentations conducted in this study. Due to the high copy number (about 50 copies per chromosome) (2, 11), this vector system was superior to a more stable low-copy-number vector system replicating via a theta mechanism. The same cassette with P_{manP} and the eGFP gene as used in pMW168.1 was inserted into a pBS72-derived plasmid with a copy number of between 5 and 10 copies (39). Cells with this new vector, pMW483.1 (see Fig. S1 in the supplemental material), proved to be more stable, and within 65 generations, about 80% of cells still carried the vector (see Fig. S2 in the supplemental material). However, the production of eGFP in TQ356/pMW483.1 was only about 30% of that of TQ356/pMW168.1 (data not shown).

Future projects will focus on evaluating the mannose expression system for proteins to be secreted into the extracellular medium.

ACKNOWLEDGMENTS

Most of the mannose used in the fed-batch fermentations was kindly provided by Lonza AG (Visp, Switzerland). We thank Andreas Freund and Salaheddine Laghrami for assistance in the computational and technical parts of the fed-batch fermentations.

REFERENCES

1. **Bertani, G.** 1951. Studies on lysogenesis. I. The mode of phage liberation by lysogenic *Escherichia coli.* J. Bacteriol. **62:**293–300.

2. **Bron, S., E. Luxen, and P. Swart.** 1988. Instability of recombinant pUB110 plasmids in *Bacillus subtilis*: plasmid-encoded stability function and effects of DNA inserts. Plasmid **19:**231–241.
3. **Chung, C. T., S. L. Niemela, and R. H. Miller.** 1989. One-step preparation of competent *Escherichia coli*: transformation and storage of bacterial cells in the same solution. Proc. Natl. Acad. Sci. U. S. A. **86:**2172–2175.
4. **Deutscher, J.** 2008. The mechanisms of carbon catabolite repression in bacteria. Curr. Opin. Microbiol. **11:**87–93.
5. **Deutscher, J., C. Francke, and P. W. Postma.** 2006. How phosphotransferase system-related protein phosphorylation regulates carbohydrate metabolism in bacteria. Microbiol. Mol. Biol. Rev. **70:**939–1031.
6. **Deutscher, J., E. Küster, U. Bergstedt, V. Charrier, and W. Hillen.** 1995. Protein kinase-dependent HPr/CcpA interaction links glycolytic activity to carbon catabolite repression in gram-positive bacteria. Mol. Microbiol. **15:** 1049–1053.
7. **Fujita, Y., Y. Miwa, A. Galinier, and J. Deutscher.** 1995. Specific recognition of the *Bacillus subtilis gnt* cis-acting catabolite-responsive element by a protein complex formed between CcpA and seryl-phosphorylated HPr. Mol. Microbiol. **17:**953–960.
8. **Galinier, A., et al.** 1998. New protein kinase and protein phosphatase families mediate signal transduction in bacterial catabolite repression. Proc. Natl. Acad. Sci. U. S. A. **95:**1823–1828.
9. **Greenberg, D. B., J. Stülke, and M. H. Saier, Jr.** 2002. Domain analysis of transcriptional regulators bearing PTS regulatory domains. Res. Microbiol. **153:**519–526.
10. **Hanson, K. G., K. Steinhauer, J. Reizer, W. Hillen, and J. Stülke.** 2002. HPr kinase/phosphatase of *Bacillus subtilis*: expression of the gene and effects of mutations on enzyme activity, growth and carbon catabolite repression. Microbiology **148:**1805–1811.
11. **Harwood, C. R., and S. M. Cutting.** 1990. Molecular biological methods for *Bacillus.* John Wiley & Sons Ltd., Chichester, England.
12. **Henkin, T. M.** 1996. The role of CcpA transcriptional regulator in carbon metabolism in *Bacillus subtilis*. FEMS Microbiol. Lett. **135:**9–15.
13. **Henstra, S. A., R. H. Duurkens, and G. T. Robillard.** 2000. Multiple phosphorylation events regulate the activity of the mannitol transcriptional regulator MtlR of the *Bacillus stearothermophilus* phosphoenolpyruvate-dependent mannitol phosphotransferase system. J. Biol. Chem. **275:**7037–7044.
14. **Henstra, S. A., M. Tuinhof, R. H. Duurkens, and G. T. Robillard.** 1999. The *Bacillus stearothermophilus* mannitol regulator, MtlR, of the phosphotransferase system. A DNA-binding protein, regulated by HPr and $IICB^{mtl}$-dependent phosphorylation. J. Biol. Chem. **274:**4754–4763.
15. **Joyet, P., M. Derkaoui, S. Poncet, and J. Deutscher.** 2010. Control of *Bacillus subtilis mtl* operon expression by complex phosphorylation-dependent regulation of the transcriptional activator MtlR. Mol. Microbiol. **76:**1279–1294.
16. **Jürgen, B., T. Schweder, and M. Hecker.** 1998. The stability of mRNA from the *gsiB* gene of *Bacillus subtilis* is dependent on the presence of a strong ribosome binding site. Mol. Gen. Genet. **258:**538–545.
17. **Keggins, K. M., P. S. Lovett, and E. J. Duvall.** 1978. Molecular cloning of genetically active fragments of *Bacillus* DNA in *Bacillus subtilis* and properties of the vector plasmid pUB110. Proc. Natl. Acad. Sci. U. S. A. **75:**1423–1427.
18. **Kim, S. I., H. Y. Kim, J. H. Kwak, S. H. Kwon, and S. Y. Lee.** 2000. Cloning, overexpression and purification of *Bacillus subtilis* elongation factor Tu in *Escherichia coli*. Mol. Cells **10:**102–107.
19. **Korz, D. J., U. Rinas, K. Hellmuth, E. A. Sanders, and W. D. Deckwer.** 1995. Simple fed-batch technique for high cell density cultivation of *Escherichia coli*. J. Biotechnol. **39:**59–65.
20. **Kunst, F., et al.** 1997. The complete genome sequence of the gram-positive bacterium *Bacillus subtilis*. Nature **390:**249–256.
21. **Laemmli, U. K.** 1970. Cleavage of structural proteins during the assembly of the head of bacteriophage T4. Nature **227:**680–685.
22. **LeBlanc, D. J., L. N. Lee, and J. M. Inamine.** 1991. Cloning and nucleotide base sequence analysis of a spectinomycin adenyltransferase AAD(9) determinant from *Enterococcus faecalis*. Antimicrob. Agents Chemother. **35:** 1804–1810.
23. **Lee, S. J., J. G. Pan, S. H. Park, and S. K. Choi.** 2010. Development of a stationary phase-specific autoinducible expression system in *Bacillus subtilis*. J. Bacteriol. **149:**16–20.
24. **Lemuth, K., et al.** 2008. Global transcription and metabolic flux analysis of *Escherichia coli* in glucose-limited fed-batch cultivations. Appl. Environ. Microbiol. **74:**7002–7015.
25. **Lorca, G. L., et al.** 2005. Catabolite repression and activation in *Bacillus subtilis*: dependency on CcpA, HPr, and HprK. J. Bacteriol. **187:**7826–7839.
26. **Michel, J. F., and J. Millet.** 1970. Physiological studies on early-blocked sporulation mutants of *Bacillus subtilis*. J. Appl. Bacteriol. **33:**220–227.
27. **Ming, Y. M., Z. W. Wei, C. Y. Lin, and G. Y. Sheng.** 2010. Development of a *Bacillus subtilis* expression system using the improved P*glv* promoter. Microb. Cell Fact. **9:**55.
28. **Nguyen, H. D., et al.** 2005. Construction of plasmid-based expression vectors for *Bacillus subtilis* exhibiting full structural stability. Plasmid **54:**241–248.
29. **Phan, T. T., H. D. Nguyen, and W. Schumann.** 2006. Novel plasmid-based expression vectors for intra- and extracellular production of recombinant proteins in *Bacillus subtilis*. Protein Expr. Purif. **46:**189–195.
30. **Postma, P. W., J. W. Lengeler, and G. R. Jacobson.** 1993. Phosphoenolpyruvate:carbohydrate phosphotransferase systems of bacteria. Microbiol. Rev. **57:**543–594.
31. **Reizer, J., et al.** 1999. Novel phosphotransferase system genes revealed by genome analysis—the complete complement of PTS proteins encoded within the genome of *Bacillus subtilis*. Microbiology **145:**3419–3429.
32. **Reizer, J., and A. Reizer.** 1996. A voyage along the bases: novel phosphotransferase genes revealed by *in silico* analyses of the *Escherichia coli* genome. Res. Microbiol. **147:**458–471.
33. **Sambrook, J., E. F. Fritsch, and T. Maniatis.** 1989. Molecular cloning: a laboratory manual. Cold Spring Harbor Laboratory, Cold Spring Harbor, NY.
34. **Schallmey, M., A. Singh, and O. P. Ward.** 2004. Developments in the use of *Bacillus* species for industrial production. Can. J. Microbiol. **50:**1–17.
35. **Schumann, W.** 2007. Production of recombinant proteins in *Bacillus subtilis*. Adv. Appl. Microbiol. **62:**137–189.
36. **Spizizen, J.** 1958. Transformation of biochemically deficient strains of *Bacillus subtilis* by deoxyribonucleate. Proc. Natl. Acad. Sci. U. S. A. **44:**1072–1078.
37. **Stammen, S., et al.** 2010. High-yield intra- and extracellular protein production using *Bacillus megaterium*. Appl. Environ. Microbiol. **76:**4037–4046.
38. **Sun, T., and J. Altenbuchner.** 2010. Characterization of a mannose utilization system in *Bacillus subtilis*. J. Bacteriol. **192:**2128–2139.
39. **Titok, M. A., et al.** 2003. *Bacillus subtilis* soil isolates: plasmid replicon analysis and construction of a new theta-replicating vector. Plasmid **49:**53–62.
40. **Tjalsma, H., et al.** 2004. Proteomics of protein secretion by *Bacillus subtilis*: separating the "secrets" of the secretome. Microbiol. Mol. Biol. Rev. **68:** 207–233.
41. **Tobisch, S., D. Zühlke, J. Bernhardt, J. Stülke, and M. Hecker.** 1999. Role of CcpA in regulation of the central pathways of carbon catabolism in *Bacillus subtilis*. J. Bacteriol. **181:**6996–7004.
42. **Warner, J. B., and J. S. Lolkema.** 2003. CcpA-dependent carbon catabolite repression in bacteria. Microbiol. Mol. Biol. Rev. **67:**475–490.
43. **Wegerer, A., T. Sun, and J. Altenbuchner.** 2008. Optimization of an *E. coli* L-rhamnose-inducible expression vector: test of various genetic module combinations. BMC Biotechnol. **8:**2.
44. **Weickert, M. J., and G. H. Chambliss.** 1990. Site-directed mutagenesis of a catabolite repression operator sequence in *Bacillus subtilis*. Proc. Natl. Acad. Sci. U. S. A. **87:**6238–6242.
45. **Wilms, B., et al.** 2001. High-cell-density fermentation for production of L-N-carbamoylase using an expression system based on the *Escherichia coli rhaBAD* promoter. Biotechnol. Bioeng. **73:**95–103.
46. **Yanisch-Perron, C., J. Vieira, and J. Messing.** 1985. Improved M13 phage cloning vectors and host strains: nucleotide sequences of the M13mp18 and pUC19 vectors. Gene **33:**103–119.